RSC Advances

PAPER

View Article Online
View Journal | View Issue

Cite this: *RSC Adv.*, 2015, **5**, 45284

A bio-friendly, green route to processable, biocompatible graphene/polymer composites†

E. Murray,*[ab] S. Sayyar,[a] B. C. Thompson,[ac] R. Gorkin III,[a] D. L. Officer[a] and G. G. Wallace[a]

Received 21st April 2015
Accepted 12th May 2015

DOI: 10.1039/c5ra07210g

www.rsc.org/advances

Graphene-based polymer composites are a very promising class of compounds for tissue engineering scaffolds. However, in general the methods of synthesis are environmentally hazardous and residual toxic materials can affect the biocompatibility significantly. In this paper a simple, scalable, environmentally-friendly, microwave-assisted synthesis is described that results in conducting graphene/polycaprolactone composites that retain the processability and biocompatibility of the pristine polymer without introducing possibly hazardous reducing agents. Composites of polycaprolactone and graphene oxide were synthesised in a single step by the ring-opening polymerisation of ε-caprolactone in the presence of dispersed graphene oxide nanosheets under microwave irradiation. The graphene oxide provides a nucleation centre for the crystallisation of the polymer resulting in polymer-functionalised nanosheets. During polymerisation, the graphene oxide was also reduced to conducting graphene. The resulting graphene/polymer composites were comparable to composites prepared by blending previously highly chemically reduced graphene into polycaprolactone, and they could be easily dispersed in a number of solvents or melt extruded for further processing. These three-dimensional melt extruded materials showed excellent biocompatibility and are promising substrates for tissue engineering scaffolds.

Introduction

Modern tissue engineering techniques seek to replace traditional medical procedures that require the repair or replacement of tissues by providing three-dimensional scaffolds on which cells can proliferate and develop into viable tissue. The scaffolds provide structural support while the cells regenerate to repair the damaged tissue and then ideally degrade or erode without harming the resulting tissue. Graphene has great promise for use in tissue engineering but lacks processability and the required mechanical properties to produce scaffolds solely from graphene.[1,2] Due to the versatility, easy functionalisation and biocompatibility of biopolymers, composites where graphene is dispersed in a polymer matrix can overcome most of these issues and are ideal scaffold materials.[1,3–5]

One other major advantage of using graphene in biocomposites is the electrical conductivity inherent in graphene sheets.[2,6,7] It has been shown that electrical stimulation during tissue growth can improve the growth of electro-responsive cells such as nerve and muscle cells.[8] Advances in the field of this electrically stimulated tissue engineering rely on the identification and development of novel electrode materials that are processable, electrochemically stable (having a wide potential window) and biocompatible.[8] We have recently shown that graphene/biopolymer,[5] especially graphene/polycaprolactone,[2,9] composites have the potential to fulfil such criteria as they show very large improvements in mechanical strength and conductivity while retaining the biocompatibility and processability of the polymer. However, these composites relied on a multi-step process that required the reduction of graphene oxide (GO) and redispersion of the resulting graphene prior to the composite synthesis.[5,6]

In addition to the introduction of further steps to the composite synthesis, the traditional methods used to reduce graphene oxide to conducting graphene before polymer blending have a number of drawbacks. Chemical reduction using reducing agents such as hydrazine,[7] hydroiodic acid in acetic acid[10] and sodium hydrosulphite[11] are routinely used to reduce GO to graphene, however these reagents are highly toxic, cannot easily be used in large quantities and require very thorough washing protocols for biomaterial synthesis. Physical reduction methods, such as hydrogen plasma[12] and rapid thermal treatment[13] were developed in order to eliminate the need for toxic reducing agents but these methods are very low-yielding and energy-intensive, again limiting their use.

[a]*ARC Centre of Excellence for Electromaterials Science (ACES), Intelligent Polymer Research Institute, AIIM Facility, Innovation Campus, University of Wollongong, NSW 2522, Australia. E-mail: emurray@ntu.edu.sg*

[b]*Institute for Sports Research, Nanyang Technological University, 50 Nanyang Ave, Singapore 639798, Singapore*

[c]*School of Mechanical and Aerospace Engineering, Nanyang Technological University, 50 Nanyang Ave, Singapore 639798, Singapore*

† Electronic supplementary information (ESI) available: Cyclic voltammetry, TGA derivative curves, cell density images and plots. See DOI: 10.1039/c5ra07210g

Recently, it has been shown that microwave irradiation is a quick and convenient alternative to flash heating methods[14,15] and can produce highly reduced conducting graphene. However, these reduced graphene sheets have the downside that they are insoluble or subject to restacking in solution, rendering post-reduction solution-based processing ineffective. In order to overcome some of these limitations polymer matrices, such as polycaprolactone (PCl), have been used as effective agents for the stabilisation of pre-reduced graphene oxide nanosheets in solution.[9,16] Combining microwave reduction, dispersion of reduced graphene and the polymerisation of the polymer matrix would eliminate a number of synthesis steps, reduce hazardous or toxic by-products and result in well-dispersed integrated materials.[3,14,17]

In this work, graphene/polycaprolactone composites (PCl–rGO) are produced when graphene oxide nanosheets are reduced during the microwave assisted ring-opening polymerisation of caprolactone. This results in a composite with well-dispersed conducting graphene sheets covalently attached to a polymer matrix that can then be easily dispersed into an appropriate solvent or melt processed using additive manufacturing techniques. These materials are compared to previously developed and published graphene/polycaprolactone composites[9] produced by blending an extensively chemically reduced and mechanically exfoliated graphene dispersion (CCG) in *N*,*N*-dimethylformamide (DMF) into a polycaprolactone matrix.

This simultaneous reduction/polymerisation removes the need for time-consuming, multi-step processes and harsh reducing materials, producing materials that are well dispersed and without harmful residues or toxic waste products. This is observed in the biocompatibility of the PCl–rGO composites which is examined by observing the adherence and proliferation of fibroblast cells on both the bulk composite and three-dimensional scaffolds produced by additive manufacturing.

Experimental

Materials

ε-Caprolactone (97%), *N*,*N*-dimethylformamide, Dulbecco's modified Eagle's medium (DMEM), methanol, dichloromethane, tin(II) ethylhexanoate (95%), H_2SO_4 and triethylamine were sourced from Sigma-Aldrich and used as received. Milli-Q water with a resistivity of 18.2 m Ω cm^{-1} was used in all preparations.

Preparation of DMF dispersed reduced graphene oxide (rGO). An exfoliated GO (0.05%) dispersion[6] was extensively chemically reduced with hydrazine and ammonia at 90 °C for 4 hours followed by a neutralisation with aqueous H_2SO_4 (5%) at room temperature, filtration and drying *in vacuo* resulting highly reduced CCG. The agglomerated CCG powder was redispersed in DMF using triethylamine by vigorous and extensive ultrasonication. The resulting supernatant is stable for several months without any agglomeration. Full details have been published separately.[6]

Preparation of polycaprolactone (PCl). The microwave-assisted polymerization of pure PCl was carried out in a CEM Discover 2.45 GHz microwave oven. In a standard synthesis, 5 ml of ε-caprolactone was mixed with 10 μl of tin 2-ethylhexanoate in a flask that was evacuated then purged with nitrogen. The mixture was reacted under flowing nitrogen using microwave irradiation (100 W max) at a constant temperature of 140 °C. The chain length could be easily varied by changing the reaction time, with longer reaction times yielding longer polymers. The crude solid product was dissolved in dichloromethane and precipitated in cold methanol, filtered and dried in a vacuum oven at 50 °C.

Sample preparation

Microwave preparation of reduced graphene oxide/polycaprolactone (PCl–rGO) composites. PCl–rGO composites of 0.1, 1 and 10% wt graphene were prepared by sonicating an appropriate volume of a 1.5% wt/vol aqueous solution of graphene oxide in ε-caprolactone until well dispersed. The solvent was reduced to <5 ml and sonicated until well dispersed. Following the addition of tin 2-ethylhexanoate the reaction vessel was evacuated then purged with nitrogen. The mixture was heated at a slow rate using microwave irradiation (100 W max) while removing the water using a Dean–Stark apparatus and reacted under flowing nitrogen at a constant temperature of 140 °C for 1 hour. The PCl–rGO composites were then precipitated in cold methanol, filtered and dried in a vacuum oven at 50 °C.

Preparation of chemically converted graphene/polycaprolactone (PCl–CCG) composites. Graphene/polycaprolactone binary mixtures were prepared by mixing polycaprolactone in an appropriate amount of a 0.5 mg ml^{-1} stable solution of DMF-dispersed graphene at 75 °C for 3 hours before cooling to room temperature. The polymer blends were then precipitated in cold methanol, filtered and dried in a vacuum oven at 50 °C.[9]

3D printing. PCl–rGO were printed by hot melt extrusion using a commercial bioprinting system (4th generation 3D-Bioplotter Envisiontec, Germany). To prepare for printing, premade PCL–rGO was loaded into a steel hopper which was sealed and inserted into a hot-melt head of the machine. The material was then heated until molten (90–100 °C) and allowed to stand for ~20 minutes in order to equilibrate the system. The system was then pressurized and readied for printing. A typical pilot three-dimensional structure for cell growth and tissue engineering was investigated where a porous mesh design was created using Envisiontec software and printed with several crisscrossing layers (with a 90 degree shift between layers) extruded from a 0.4 mm nozzle. The resulting crosshatched multi-layer scaffold structure has pore sizes of approximately 1 mm.

Characterization

Structural characterisation. Powder samples of polymer composites for X-ray diffraction, Raman spectroscopy and thermal analyses were prepared by precipitating the material in question in cold methanol and extensive air and vacuum drying at 50 °C. Thermal gravimetric analysis (TGA) was performed

using a TGA Q500 (TA Instruments) with a heating rate of 10 °C under a nitrogen atmosphere. Differential scanning calorimetric (DSC) analysis was performed on a DSC Q100 (TA Instruments). X-ray powder diffraction (XRD) analysis was performed using GBC MMA diffraction equipment (GBC Scientific Equipment Pty Ltd, Australia) equipped with Cu-Kα radiation. Raman spectra were recorded on a Jobin Yvon Horiba HR800 Raman microscope using a 632 nm laser line and a 300-line grating. Dynamic light scattering (DLS) measurements were performed on a Malvern zetasizer and the resulting data were processed using the proprietary software. DLS samples of the polymer composite were prepared by dissolving PCl–rGO in an appropriate solvent, in this case dichloromethane, at an approximate concentration of 10 mg ml^{-1} by 30 seconds sonication. Similar results were observed for the PCl–CCG sample. Suspensions of highly chemically reduced non-stabilised graphene were achieved by extensive sonication (7+ hours) in *N*,*N*-dimethylformamide at a concentration of 0.5 mg ml^{-1}. Cyclic voltammetry was performed on a coated platinum working electrode in 0.1 M aqueous KNO_3 with an Ag/AgCl reference at 100 mV s^{-1}.

***In vitro* biocompatibility.** Assessment of biocompatibility was performed by culture of a rat fibroblast cell line (L-929) on films and printed scaffolds made from the material. A Pico Green assay was used to compare the number of cells after 4 days of growth on the materials to growth on tissue culture plastic. In short, cells were seeded at 1500 cells per cm^2 in a 12 well plate coated with PCl–rGO and PCl, and incubated for 4 days before the media was removed, and cells lysed in 0.1% sodium dodecyl sulphate in 1× Tris–EDTA buffer. The amount of DNA in the lysed cell solutions was analysed by addition of the Pico Green reagent, as per the manufacturer's instructions, and the fluorescence of the solutions converted to a cell number using a standard curve solution of known cell density.

For imaging of cells on the scaffold surfaces, L-929 cells were seeded onto 2 × 2 cm 6–8 layer scaffolds in 6 well plates at approximately 1×10^6 cells per ml in 1 ml and allowed to attach for 30 minutes in the incubator before the media in the well was topped up to 2 ml. The scaffolds were returned to the incubator for 4 days before fixation of the cells with 3.7% paraformaledhyde in PBS and staining with Alexa488-phalloidin (Life Technologies) and 4′,6-diamidino-2-phenylindole (DAPI) (Life Technologies), and imaging using a Leica TCS-SP5 confocal microscope, and a Leica DM IL LED. Z-stacks were acquired on the confocal microscope with a slice height of 1.1 μm were taken over 250 μm height and Imagesurfer 1.24 was used to render 3D isosurface images of the cells growing on the scaffolds.

Results and discussion

The microwave synthesis of polymer composites provides an efficient, scalable route to biopolymer composites with reaction times reduced to a fraction of those required when using standard heating methods. Microwave radiation has also been shown to reduce graphene oxide without the use of harmful chemical reducing agents but on a timescale much shorter than that of the polymerisation (a number of seconds), ensuring that the growing polymer chain attaches to peripheral carboxyl groups following reduction of the basal defects. This indeed seems to be the case with the microwave-assisted polymerisation of ε-caprolactone in the presence of graphene oxide, which easily produces well dispersed reduced graphene/polycaprolactone (PCl–rGO) at low initial GO concentrations (<2% wt GO). These composites were compared to materials produced by blending extensively reduced CCG into a polycaprolactone matrix at similar graphene concentrations. Increasing the initial concentration of graphene in the microwave synthesis to 10% resulted in poor dispersion of the nanosheets and localised heating during reaction causing poor polymerisation.

Raman spectra of GO, CCG and the microwave-reduced graphene/polycaprolactone composite, 1% PCl–CCG, in this case with 1% graphene, were obtained (Fig. 1). As expected all three spectra are dominated by the D (1250–1450 cm^{-1}) and G (1530–1670 cm^{-1}) bands.[7,18] For GO, the D and G bands are located at 1343 and 1606 cm^{-1} respectively. A shift to 1327 and 1599 cm^{-1} in the microwave synthesised PCl–rGO composite indicates an increase in the number of graphene π-bonds and is very similar to that observed for graphene (CCG) after having been chemically reduced and exfoliated using hydrazine and extensive sonication.[2,6] The intensity ratio of the D and G bands changes from 1.13 for GO to 1.47 for 1% PCl–rGO approaching the 1.61 observed for CCG. Minor peaks due to the polymer are also observable in the 1% PCl–rGO spectrum.

The XRD spectrum of GO (Fig. 2) is dominated by an intense, peak at $2\theta = 10°$ (*d*-spacing of about 8.35 Å) indicating a large interlayer distance due to surface impurities such as hydroxides and epoxides. In the spectrum of the polymer composites, the peaks at $2\theta = 21$ and 24° can be assigned to (110) and (200) planes respectively, of an orthorhombic crystalline structures of PCl, which mask the broad weak band due to pristine, reduced exfoliated graphene sheets. The removal of the peak at 10° indicates exfoliation and reduction of GO to single or few-sheet graphene with a much reduced inter-sheet spacing. This is also

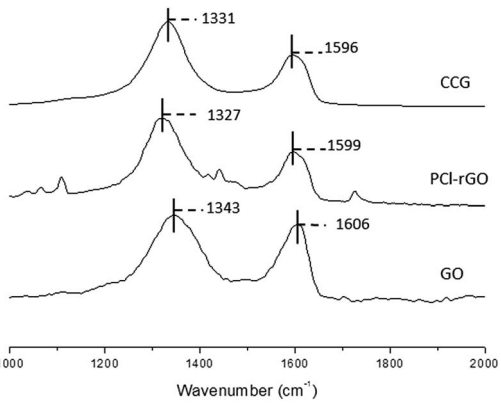

Fig. 1 Raman spectra of powder samples of graphene oxide (GO), chemically reduced graphene (CCG) and a graphene/polycaprolactone composite with 1% graphene oxide (1% PCl–rGO), showing the shift in positions and relative intensities of the D and G bands.

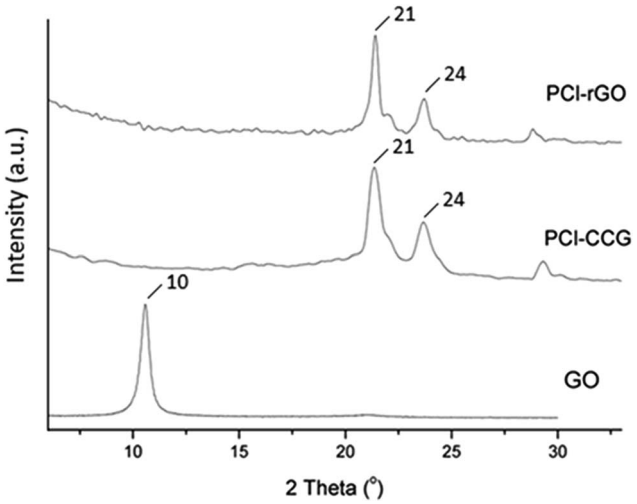

Fig. 2 X-ray diffraction (XRD) patterns of graphene oxide and graphene/polycaprolactone composites synthesised using microwave reduced graphene oxide (1% PCl–rGO) and chemically converted graphene (1% PCl–CCG).

observed in the spectra of the polymer composite produced using chemically converted and exfoliated graphene, PCl–CCG.

In the infrared spectrum of GO, the C=O stretching and deformation peaks appear at 1730 cm^{-1} and 1400 cm^{-1}, respectively (Fig. 3). The strong band at 3410 cm^{-1} is attributed to O–H stretching. After reduction by either microwave or chemical methods, the intensity of the graphene-based oxygen peaks are decreased significantly confirming the reduction of graphene oxide. The OH stretch peak is also not present showing good reduction of the graphene sheets. In PCl and PCl composites (Fig. 3), a carbonyl stretching mode can be identified at 1724 cm^{-1}, the band at 1292 cm^{-1} is assigned to the backbone C–C and C–O stretching modes in crystalline PCl and peaks at 2943 and 2866 cm^{-1} are attributed to asymmetric CH_2 stretching and symmetric CH_2 stretching, respectively.[19]

Both synthetic routes resulted in polycaprolactone functionalised graphene sheets (PCl–rGO and PCl–CCG) that were readily dispersible and stable in non-polar solvents. Fig. 4 shows the dynamic light scattering results for a 10 mg ml^{-1} solution of 1% PCl–rGO in dichloromethane. Also shown is a sample of the CCG dispersions that are the precursor to the PCl–CCG composites and have been extensively treated by ultrasonication in DMF. These dispersions have previously been shown to be a stable suspension of well-exfoliated single or small number of sheets.[6] The size intensity average plot shows a hydrodynamic radius of approximately 400 nm for the bare graphene and 1000 nm for the polymer composite.

The polymer stabilised composite (1% PCl–rGO) exhibits a narrow dispersion of sheet sizes and shows very little evidence of larger particle radii. This indicates that post-reduction, the sheets are well exfoliated and dispersed during or just prior to polymerisation allowing the polymer to grow on and stabilise single sheets. The inset is a picture of the solutions used in light scattering experiments and shows the solubility of the composite in dichloromethane with solutions of 1% PCl–rGO composite at two concentrations – 5 mg ml^{-1} and 50 mg ml^{-1}.

The thermal degradation of the polymer composites was measured using thermal gravimetry and the results are shown in Fig. 5. GO generally loses about 20–40% of its weight due to trapped moisture at approximately 100 °C followed by a second thermal event (between 200 and 900 °C) that has been assigned to the reduction of and removal of surface epoxide and hydroxide and other functionalities.[6] Chemically reduced graphene (CCG), on the other hand, is fully exfoliated and lacks significant numbers of basal defects showing only slight monotonic loss of <5% of its weight by 600 °C.[6] The thermal degradation of PCl is very dependent on chain length (from 300 to 500 °C for average chain lengths of 10 000 to 80 000 Fig. S2†) so direct comparison of the composites behaviour with a pristine polymer is difficult as the length of the graphene-anchored PCl chain from the microwave synthesis is unknown. The

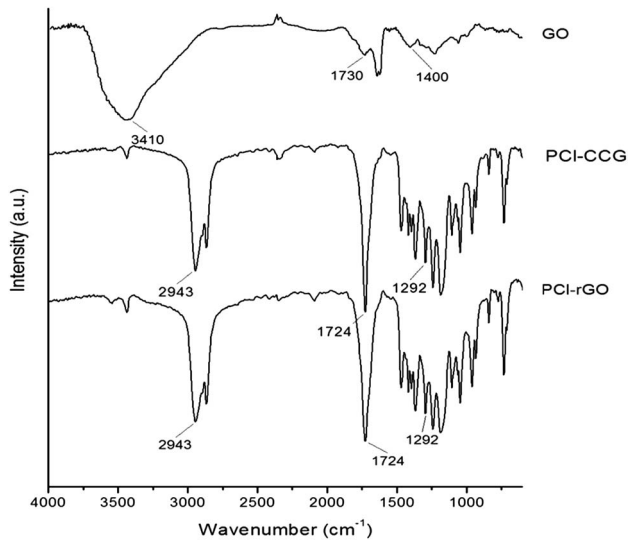

Fig. 3 Infra-red spectra of graphene oxide (GO) and two graphene/polycaprolactone composites made with graphene oxide (1% PCl–rGO) and chemically converted graphene (PCl–CCG).

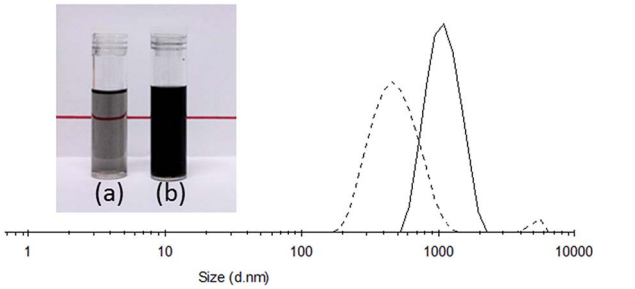

Fig. 4 Size intensity curves from the dynamic light scattering of a 1% PCl–rGO solution in dichloromethane (DCM) at 10 mg ml^{-1} (solid line) and an extensively sonicated solution of chemically converted graphene (CCG) in DMF at 0.5 mg ml^{-1} (dashed line). The inset shows DCM solutions of 1% PCl–rGO at (a) 5 mg ml^{-1} and (b) 50 mg ml^{-1}.

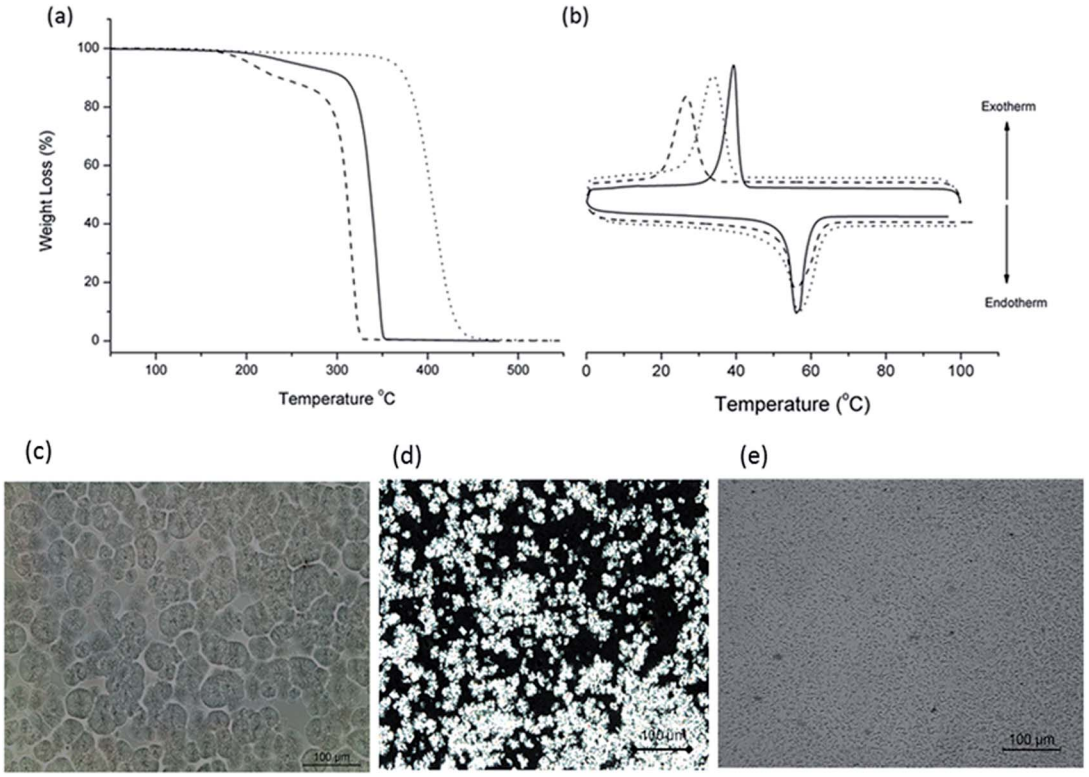

Fig. 5 (a) Thermogravimetric curves for microwave synthesised 0.1% PCl–rGO (—) 1% PCl–rGO (—) and blended 1% PCl–CCG (●●●) with 80 000 MW polycaprolactone. (b) Differential scanning calorimetry for pristine 80 000 MW polycaprolactone (—) 1% PCl–rGO (—) and blended 1% PCl–CCG (●●●). (c), (d) and (e) are polarised optical microscopy images taken below the crystallisation temperature showing the nucleation and differences in spherulite size and density of pure PCl, 1% PCl–CCG and 1% PCl–rGO respectively.

degradation of the blended PCl–CCG composite is a monotonic weight loss from 400–450 °C. In contrast, the degradation of the microwave composites with 0.1 and 1% graphene appear to be two-staged; an initial minor loss from 200–250 °C and then full degradation of the polymer (Fig. 4). This initial loss can be interpreted as resulting from either the loss of basal defects as in GO or the loss of shorter PCl chains attached to the nanosheet. However, the degradation of 10% graphene composite shows a far increased initial weight loss (Fig. S2†) which, taking into account the similar reaction conditions and resulting material properties, cannot be attributed to loss of basal defects on GO. The initial loss can thus be attributed to the degradation of shorter polymer chain lengths or very short polymer chains joining two graphene molecules as a crosslinker.

Differential scanning calorimetry shows that the melt point of the composite remains constant at 56–60 °C (Fig. 5b). This allows easy melt processing of the composite. However, the crystallisation temperature changes dramatically from 26 °C for PCl to 39 °C for a composite produced using microwave polymerisation reduction (1% PCl–rGO). This indicates that the incorporation of graphene nanosheets into the PCl affects the polymer microstructure by acting as multiple nucleation centres for crystallisation. This change in crystallisation temperature is less pronounced in composites produced by blending CCG with PCl with the crystallisation temperature of 1% PCl–CCG increasing to 35 °C (Fig. 5b).

The nucleating effect of the exfoliated GO nanosheets on the crystallization of PCl is also confirmed by polarised optical microscopy. Fig. 5c–e show polarised optical microscopy images of pure PCl, 1% PCl–CCG and 1% PCl–rGO after the samples were heated to 100 °C and allowed to cool below their respective crystallisation temperatures. The spherulites of pure PCl are much larger in size (50–100 μm) and less densely packed than the graphene containing materials leading to a large increase in nucleation density in both composite materials. As predicted by the DSC the blended material (PCl–CCG) exhibits larger spherulites (10–20 μm) than the microwave synthesised composite (PCl–rGO 2–10 μm).

In tissue engineering, cells are often seeded onto a biodegradable scaffold to promote the growth and remodelling of tissue. However, traditional methods for scaffold fabrication struggle to accurately create specific custom geometries and produce interconnected porous networks that allow for optimal tissue regrowth. 3D Bioprinting methods can overcome these limitations once a suitable scaffold matrix material is found. We have a good indication that these new materials would work with a printing system as we previously showed that covalently linked graphene/polymer composites retain the melt temperature and rheological properties (complex viscosity) of the pristine polymer required for printing, on addition of graphene.[4,9]

To that end, the viability of processing PCl–rGO composites was evaluated using a commercial bioprinting system

(4th generation 3D-Bioplotter Envisiontec, Germany). For these materials a hot melt extrusion printing method was performed. In brief the process involves heating solid materials until they are molten, and then extruding them out a nozzle on a movable gantry. 3D structures are created in a layer-by-layer fashion, where the heated extrusion solidifies on a build plate forming the first level, and subsequent layers are formed on top.

Following the incremental adjustment of various printing parameters to find the optimal settings, the composites were printed/extruded successfully in the form of scaffolds and fibres with easily controllable resolution. A typical pilot three-dimensional structure for cell growth and tissue engineering was investigated where a porous mesh design was created using Envisiontec software and printed with several crisscrossing layers (with a 90 degree shift between layers) extruded from a 0.4 mm nozzle (as seen in Fig. 6a and b). The resulting cross-hatched multi-layer scaffold structure has pore sizes of approximately 1 mm.

Biocompatibility is crucial for prospective tissue engineering scaffolds. We have already shown the biocompatibility of graphene/PCl materials with a number of cell types.[15] In order to assess the response of cultured cells *in vitro* to the microwave synthesised composites, L-929 cells were seeded onto to the flat films and scaffold structures of PCl, PCl–rGO, and PCl–rGO. The flat films were found to allow attachment and proliferation of L-929 fibroblasts, albeit at lower rates than the control surface (tissue culture plastic) alone (Fig. S2†). The results of a Pico Green assay showed that the rate of growth was slower on the PCl–rGO or PCl films and the cell population underwent 2–3 doublings on the synthesised materials, compared to 3–4 doublings on tissue culture plastic. The cell densities measured after 4 days of culture were 5400 ± 300 cells per cm^2 on PCl, 10 000 ± 2000 cells per cm^2 on 1% PCl–rGO and 19 200 ± 700 cells per cm^2 on tissue culture plastic (a cell density representing greater than 100% confluence of cells) (Fig. S2†).

Microscopy confirmed that cells adhered to and proliferated on the scaffold surfaces, forming good focal adhesions (Fig. 7b) and covering all surfaces of the printed scaffolds (Fig. 7c), except those contacting the plate bottom. The cells grew with normal fibroblast morphology (Fig. 7) and the density of the cells increased over the 4 days of culture. A confluent layer of cells was observed to form on the tissue culture plastic underneath the scaffolds (Fig. S3†), suggesting that any differences

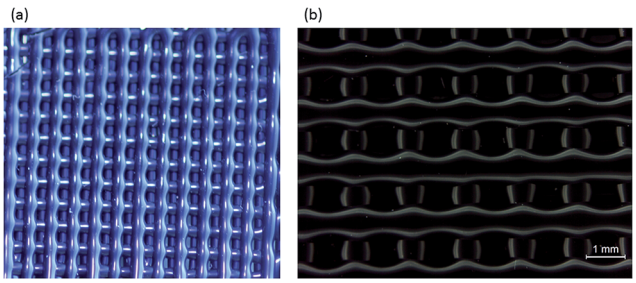

Fig. 6 Multi-layer melt extrusion printed three-dimensional porous mesh scaffold of 1% PCl–rGO.

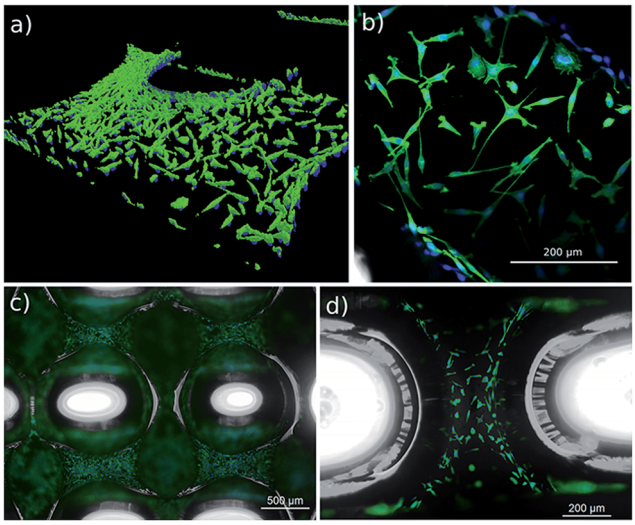

Fig. 7 Images of L-929 cells growing on a printed 1% PCl–rGO scaffold. The cytoskeleton is labelled with Alexa488-phallioin (green) and the nuclei are DAPI stained (blue). (a) shows isosurface rendering of confocal microscope images of cells growing on the scaffold, illustrating their adhesion to the side walls of the scaffold, not merely the top surfaces. Images (b–d) show fibroblast cells adhered to the scaffolds.

experienced by the growing fibroblast cells was surface-confined, and not related to any soluble factors released into the growth media. As with the 1% PCl–rGO films assessed by the Pico Green assay, the rate of L-929 cell growth was somewhat slower than that expected on tissue culture plastic alone, but the cells attached firmly, migrated and proliferated to cover the entire scaffold (Fig. S3 and S4†). The scaffolds showed no toxic effects and good adhesion of cells over all surfaces, demonstrating good acute *in vitro* biocompatibility and warranting further development of these scaffolds for *in vivo* studies.

Conclusions

This paper introduced the production of tissue engineering graphene/polymer composites using a single step reaction without the need for harsh, toxic reducing agents that could interfere with biocompatibility or leach in long term implants. Microwave irradiation was successfully used as a quick, efficient and 'green' synthesis route to produce graphene/polycaprolactone composites using both GO and CCG. During polymerisation, the GO was also reduced resulting in conducting graphene sheets (Fig. S1†) well dispersed in a polymer matrix that were comparable to the graphene sheets in the composite produced from preformed graphene using extensive physical and chemical processing. In both types of composite, the reduced graphene nanosheets functioned as nucleation centres in the crystallisation of the polymer leading to a more densely packed material. However, the solubility and melt properties of the polymer were retained resulting in a material that could be easily processed using solution and additive fabrication methods. The composite also retained the biocompatibility of the polymer resulting in very promising scaffold materials for tissue engineering of electro-responsive cells.

Acknowledgements

This work has been supported by the Australian Research Council (ARC) under Superscience and Australian Laureate Fellowship funding schemes and the Australian National Fabrication Facility (ANFF). We also acknowledge use of the facilities at the UOW Electron Microscopy Centre (EMC).

Notes and references

1 B. C. Thompson, E. Murray and G. G. Wallace, *Adv. Mater.*, 2015, DOI: 10.1002/adma.201500411.
2 H. Chen, M. B. Mueller, K. J. Gilmore, G. G. Wallace and D. Li, *Adv. Mater.*, 2008, **20**, 3557.
3 H. Hu, X. Wang, J. Wang, F. Liu, M. Zhang and C. Xu, *Appl. Surf. Sci.*, 2011, **257**, 2637.
4 S. Sayyar, R. Cornock, E. Murray, S. Beirne, D. L. Officer and G. G. Wallace, in *Advances in Materials and Processing Technologies Xv*, ed. A. K. Tieu, H. Zhu and Q. Zhu, 2014, vol. 773–774, p. 496.
5 S. Sayyar, E. Murray, B. C. Thompson, J. Chung, D. L. Officer, S. Gambhir, G. M. Spinks and G. G. Wallace, *J. Mater. Chem. B*, 2015, **3**, 481.
6 S. Gambhir, E. Murray, S. Sayyar, G. G. Wallace and D. L. Officer, *Carbon*, 2014, **76**, 368.
7 S. Stankovich, D. A. Dikin, G. H. B. Dommett, K. M. Kohlhaas, E. J. Zimney, E. A. Stach, R. D. Piner, S. T. Nguyen and R. S. Ruoff, *Nature*, 2006, **442**, 282.
8 G. G. Wallace, S. E. Moulton and G. M. Clark, *Science*, 2009, **324**, 185.
9 S. Sayyar, E. Murray, B. C. Thompson, S. Gambhir, D. L. Officer and G. G. Wallace, *Carbon*, 2013, **52**, 296.
10 I. K. Moon, J. Lee and H. Lee, *Chem. Commun.*, 2011, **47**, 9681.
11 T. Zhou, F. Chen, K. Liu, H. Deng, Q. Zhang, J. Feng and Q. Fu, *Nanotechnology*, 2011, **22**, 045704.
12 A. Dato, V. Radmilovic, Z. Lee, J. Phillips and M. Frenklach, *Nano Lett.*, 2008, **8**, 2012.
13 H. C. Schniepp, J. L. Li, M. J. McAllister, H. Sai, M. Herrera-Alonso, D. H. Adamson, R. K. Prud'homme, R. Car, D. A. Saville and I. A. Aksay, *J. Phys. Chem. B*, 2006, **110**, 8535; H. C. Schniepp, D. A. Saville and I. A. Aksay, *J. Am. Chem. Soc.*, 2006, **128**, 12378.
14 W. Chen, L. Yan and P. R. Bangal, *Carbon*, 2010, **48**, 1146.
15 Y. Zhu, S. Murali, M. D. Stoller, A. Velamakanni, R. D. Piner and R. S. Ruoff, *Carbon*, 2010, **48**, 2118.
16 L. Hua, W. Kai and Y. Inoue, *J. Appl. Polym. Sci.*, 2007, **106**, 1880; W. Kai, Y. Hirota, L. Hua and Y. Inoue, *J. Appl. Polym. Sci.*, 2008, **107**, 1395.
17 M. A. Aldosari, A. A. Othman and E. H. Alsharaeh, *Molecules*, 2013, **18**, 3152.
18 V. C. Tung, M. J. Allen, Y. Yang and R. B. Kaner, *Nat. Nanotechnol.*, 2009, **4**, 25; S. Villar-Rodil, J. I. Paredes, A. Martinez-Alonso and J. M. D. Tascon, *J. Mater. Chem.*, 2009, **19**, 3591.
19 T. Elzein, M. Nasser-Eddine, C. Delaite, S. Bistac and P. Dumas, *J. Colloid Interface Sci.*, 2004, **273**, 381.

